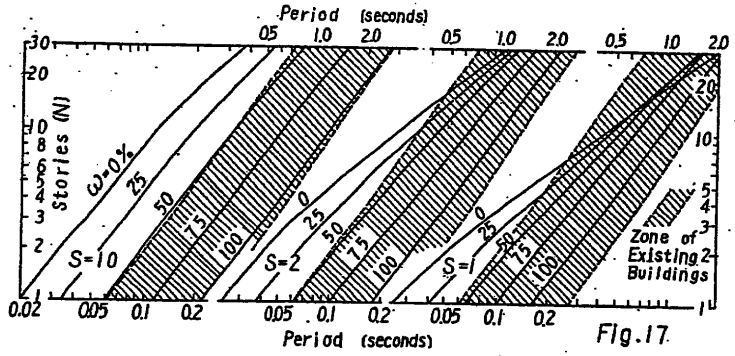

Fig.17

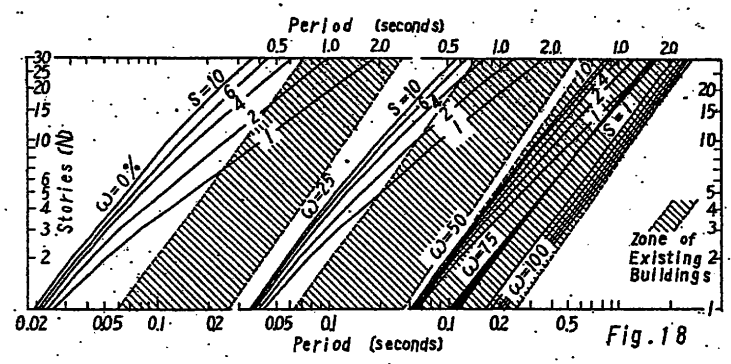

Fig.18

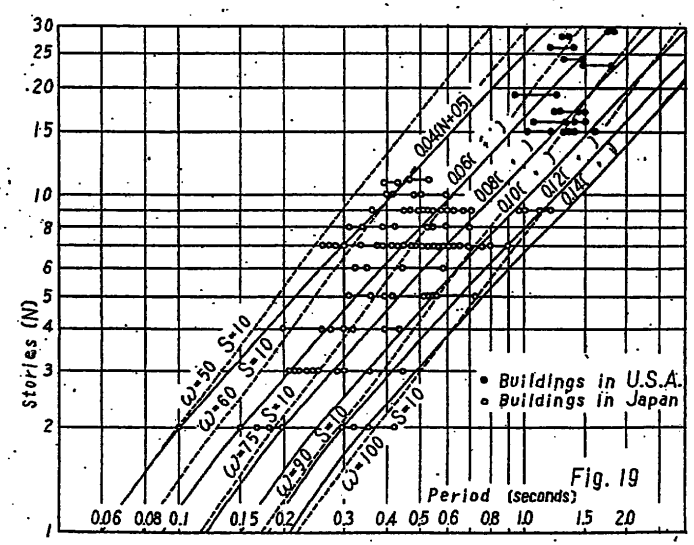

Fig. 19

DAMPING IN COMPOSITE STRUCTURES

by Lydik S. Jacobsen*

ABSTRACT

Damping in composite structures occurs mainly at their various joints. A discussion of the adequacy of the equivalent viscous friction concept is followed by an attempt to discern simple geometrical design principles for an idealized relationship between load and deflection in a hysteretic but non-deteriorating joint. A comparison of performances of idealized joints with those of actual joints is made.

INTRODUCTION

From the point of view of resistance to earthquake loads the presence of a relatively large amount of damping is highly desirable in a structure, because it dissipates the vibrational energy transmitted by the quake to the structure, and it counteracts the generation of large structural amplitudes during quasi-resonance conditions.

Since the internal damping in the elastic ranges of many building materials is small, we shall be concerned mainly with damping in the elastic-plastic ranges of the materials, especially in the regions of limited extent, that is, at locations of plastic hinges and at spots where strain concentrations are present. This at once focuses our attention on structural joints of the pinned, bolted, riveted, nailed and generally clamped types. These may be classified as intentional, designed joints in distinction to unintentional or accidental ones as: cracks due to shrinkages, settlements, dislocations or other external force applications.

It is significant that an extremely small amount of frictional sliding between clamped surfaces as well as plastic deformations in very limited regions of strain concentration will affect the damping properties of a structure greatly. Unfortunately almost no determinations of structually dynamic damping properties have been made, primarily because it is very difficult to do. Our studies therefore, must be based mainly on static tests, but even then it is regrettable that so few tests have been carried out for several cycles of loading in alternate directions.

The question immediately arises as to how well the static behavior of a structure, loaded in alternate plus and minus directions, will correlate with its dynamic behavior. Nearly all investigators will agree that the dynamic stiffness and strength are usually found to be greater than the static, but just how much? Estimates will vary from a few per cent up to as much as forty.

Wilbur and Hansen[1] experimenting statically and dynamically on reinforced concrete beams, have come to the conclusions that for so-called long

*Professor of Mechanical Engineering, Chairman of Department, Stanford University, California, U.S.A.

Proc. 2nd World Conference on Earthquake Eng., 1965

duration force applications, (10 seconds) and for short duration (50 milliseconds) the beams' resistances were from 0 to 6 per cent and from 15 to 30 per cent larger than their static resistances, moreover, the work integrals (total work of damping) for the durations were about 15 and 30 per cent larger respectively than for static loads. It is purely conjectural as to how a still shorter duration of force application might affect the beams. Since their fundamental periods were in the order of 35 milliseconds, the short duration was about 40 to 50 per cent longer than the beams' periods. This raises the point of distinguishing the truly inherent dynamic resistance and damping properties of the materials apart from the apparent resistance and damping attributable to the specific vibrating properties of the beams as "tuned in" to any time duration of force application.

Without introducing material constants that are functions of the dynamics itself the complexity of non-linear, dissipative systems is great enough. Consequently we shall be content - temporarily - with the assumption that the material constants for static behavior are similar and not widely different from those for dynamic loadings. This includes the elastic, the elastic plastic, and the true plastic stages.

EQUIVALENT DAMPING CAPACITY

Unlike a clean laboratory test specimen of a homogeneous material, a composite structure may have several localized strain phenomena and slippages between its clamped surfaces. Accordingly its static load distortion curve will depict the total effect of the composite element's individual contributions. In most cases a truly elastic range therefore is very short and a hysteretic effect is appreciable. The practical relation of the shape and size of a composite structure's static hysteresis loop to a dynamical damping quantity is a debatable one in which it is usually necessary to sacrifice accuracy to expediency.

It is easy to demonstrate that for some types of friction forces, as for instance rubbing or Coulomb forces, an equivalent viscous damping force is a relatively poor approximation. Nevertheless most investigators prefer to select the concept of equivalent viscous damping to represent the damping properties of any vibrating system, linear or not. It is clear that for small damping values and for almost linear systems the equivalent viscous damping is likely to be justifiable, but for strongly non-linear systems with non-viscous friction an equivalent viscous damping may become almost meaningless.

Figure 1a shows a frictionless linear system whose restoring force F_r is equal to kx. The maximum elastic potential energy E_p is then equal to $\frac{1}{2}kX^2$, Figure 1b. Since the sum of potential and kinetic energy E_k is constant and equal to $\frac{1}{2}kX^2$, the kinetic energy variation with x appears in Figure 1c. The corresponding velocity $\dot{x}$ then becomes:

$$\dot{x} = \sqrt{\frac{k}{m}}\, X \left[1 - \left(\frac{x}{X}\right)^2\right]^{\frac{1}{2}}$$

A plot of the velocity against x gives the ellipse shown in Figure 1d. If set into vibration with the amplitude X, this system will keep vibrating indefinitely.

Imagine now that the described vibration system is influenced by a viscous damping force equal to $c\dot{x}$ and that an alternating external force keeps it vibrating with the same amplitude as before at its natural frequency. The damping force will then be the semi-ellipse depicted in Figure 1c. The frictional work done by this force is supplied by the alternating external force; it will be equal to the area of the semi-ellipse or to $W_c = \frac{\pi}{2} c \sqrt{\frac{k}{m}}\, X^2$. Since the maximum potential energy E_p as represented by the triangular area of Figure 1a gives the relation $X^2 = 2E_p/k$, we find that:

$$\frac{c}{2\sqrt{km}} = \frac{1}{2\pi}\,\frac{W_c}{E_p}$$

Now, the quantity $2\sqrt{km}$ is the critical damping coefficient c_{cr} of the linear system. Consequently the damping coefficient ratio ν is:

$$\nu = \frac{c}{c_{cr}} = \frac{1}{2\pi}\,\frac{W_c}{E_p}$$

Thus, if the semi-elliptical and the triangular areas are equal, $W_c = E_p$, the value of ν will be 0.159.

Finally, Figure 1f shows the combined restoring force, viscous friction force diagram for the half cycle with positive displacements. It is seen that the dotted straight line, kx, may be thought of as the "skeleton" of the combined curves.

Figure 2a shows the frictionless non-linear vibrating system whose restoring force F_r varies as the fourth root of x. At $x = X$ the restoration is made to have the identical maximum force value, namely kX, with the system in Figure 1a. In this case the maximum potential energy is larger than before, namely $4/5\ kX^2$, Figure 2b. The kinetic energy and the corresponding velocity distribution curves are shown in Figures 2c and 2d respectively. This non-linear system, if started with an amplitude X, will also continue to vibrate indefinitely at the natural frequency corresponding to its amplitude.

We now imagine that this system is influenced by viscous damping equal to $c\dot{x}$ and that a suitable alternating force keeps it vibrating with the amplitude X at its appropriate natural frequency. Figure 2e then depicts the damping force, a modified semi-ellipse. The area enclosed by the curve represents the frictional work for one half cycle; it is equal to:

$$W_c = 1.13\,\frac{\pi}{2}\, c \sqrt{\frac{k}{m}}\, X^2$$

Replacing X^2 by its value from Figure 2b, namely $5/4\ E_p/k$, we find that

$$\frac{c}{2\sqrt{km}} = \frac{1.42}{2\pi}\,\frac{W_c}{E_p} = \nu_{eq}$$

We may therefore speak of an equivalent viscous damping coefficient ratio ν_{eq} which will be 42 per cent larger than for the same W_c/E_p ratio of the linear case.

The combined restoring force plus friction force curve for the half cycle with positive displacements is shown in Figure 2f. In this case the restoration force curve, dotted, may be thought of as the "skeleton" of the combined curve.

Similar calculations for an increasing restoring force varying as the 3/2 power of x, are shown in Figures 3a, b, c, d, e and f. They give:

a value about 3 per cent lower than for the linear case.

The above demonstration illustrates the fact that the concept of an equivalent viscous damping is not easily applied to arbitrary non-linear systems, because their critical damping coefficient has no simple relation to the linear one of $2\sqrt{km}$. In concluding this discussion we may say that for a linear or non-linear system influenced by non-viscous damping, the problem of finding an equivalent viscous damping coefficient ration ν_{eq} involves additional debatable assumptions. With this reservation in mind we nevertheless shall speak of ν_{eq} as expressible by the rough formula:

$$\nu_{eq} \approx \frac{1}{2\pi} \frac{\text{Frictional Work Area}}{\text{Work Area under Skeleton}} \equiv \frac{1}{2\pi} \frac{\Delta W}{W}$$

This definition introduces an element of "artistic judgment because in many practical cases the skeleton is not known, accordingly the work area W can be conjectured only.

From a philosophical point of view it must be admitted that it is highly artificial to separate restoring forces and friction forces in vibrational systems where the hysteretic effect is a function of displacement only.

REMARKS ON DETERIORATION

Since the elastic plastic strain regions of most materials exhibit the phenomenon of deterioration a few words should be said about it. A priori it is possible to imagine joints without deterioration. Thus a pure sliding friction joint of the type that Pian, Hallowell and Bisplinghoff[2] studied and tested will show almost no deterioration. It is true that after many load changes the coefficients of friction between the clamped surfaces may diminish, but as long as nothing fails - in the sense of breaking as well as in the sense of releasing clamping forces - the sliding friction joint is almost non-deteriorating for a reasonable number of load changes. The same argument can be made for joints in which the plastic deformations are not too large and do not influence clamping forces between surfaces. Of course, if the strain concentrations are severe enough to cause local breaks, deterioration is unavoidable.

IDEALIZED GEOMETRIC LOAD DEFLECTION CURVES

A simplified, behavioristic representation of hysteretic, non-deteriorating joints will now be proposed. It is mainly applicable to softening joints, and it is based on the following three debatable premises:

I A primitive or "virgin" load distortion curve is known for a gradually increasing distortion.

II An initial, constant load-distortion slope exists for a finite distortion.

III When a load is diminished, the load distortion trajectory is a circle of constant radius with an initial slope equal to the one at zero load.

Since the study will be geometrical and greatly concerned with areas it is desirable to use dimensionless plotting and to choose the plotting scales so as to have the initial load distortion slope equal to unity. We call the dimensionless force coordinate ϕ and the dimensionless distortion coordinate δ ; the units on both axes will be in terms of multiples of ϕ and δ at the initial proportional limit.

BI-LINEAR JOINTS

A bi-linear, elastic-plastic joint with slopes of unity and zero is shown in Figure 4a. It is assumed that any initial load is smaller than unity so that it will be located on the line 4 - 0 - 1. If the distortion δ increases to +2 units ϕ will remain at one unit and the terminal position is at 2. If the distortion now decreases, ϕ will decrease along the circular trajectory 2 to 3 where ϕ will be zero. The radius of the trajectory is such as to give an initial return slope of unity at station 2, and pass through station 4, the point where ϕ and δ both are -1. It is seen that a permanent set of 0 - 3 occurs at station 3.

If at station 3 the δ is now increased, ϕ will increase along another circular trajectory, but of the same radius as before; to station 2, thereby enclosing a small hysteretic loop. Next, if δ is decreased to -1, ϕ moves along the first circular trajectory to station 4 where it has the value of -1. The maximum hysteretic loop, enclosed by the two circular arcs of constant radius, involves stations 2 - 3 - 4 - and 2. Moreover, if at station 2, δ is decreased from +1 to -2 the trajectory will be along 2 - 3 - 4 - 5. Finally a change in δ from -2 to +1 will move ϕ along 5 - 1. In this diagram δ has varied only between ± 2 and ϕ between ± 1.

A suitable skeleton for the loop 2 - 3 - 4 - 2 is a straight line, consequently its triangular area is well defined; this gives ν_{eq} close to 0.05. The skeleton for the loop 1 - 2 - 3 - 4 - 5 - 1 is more problematic. If we take the triangular area under the straight line from 0 to 2, ν_{eq} becomes about 0.12; but if we take the area under a straight line from 0 to midway between stations 1 and 2, ν_{eq} will increase to about 0.15.

Figure 4b shows δ varying between ± 4. The radius of the appropriate circular trajectory again is determined by having unit slope at station 7 and by letting it pass through the point where $\delta = \phi = -1$. However, in this case it intersects the $\phi = -1$ line at station 10.

Consequently the largest hysteretic area will be bounded by the circular arcs 7 - 8 - 9 - 10 - 7. This area is considerably larger than the largest similar area under Figure 4a; it is primarily due to the larger δ range of approximately 5 units. If the loop's δ range is reduced to 3 units, the loop 7 - 8 - 9 - 7 results. The suitable skeletons for loops 7 - 8 - 9 - 10 - 7 and for 7 - 8 - 9 - 7 are obviously straight lines; they give ν_{eq} = 0.12 and 0.07 respectively. Again, the skeleton for the entire loop 6 - 7 - 10 - 17 - 6 is problematic. If triangular areas under the straight lines 0 - 7, and under line 0 to midway between 6 and 7 are selected, we obtain ν_{eq} = 0.33 and 0.52 respectively. Finally, Figure 4c shows the ϕ, δ plot for a δ range of ± 8. The hysteretic loop 15 - 16 - 17 - 15 is formed by circular arcs whose equal radii are determined by letting the descending one have unit slope at station 15 and pass through station 18. The ν_{eq} of this loop is about 0.06. Loop 15 - 16 - 15 - spans the same range of 3 δ as loops 2 - 3 - 4 - 2 and 7 - 8 - 9 - 7; its ν_{eq} is about 0.05. A consideration of the large loop 14 - 15 - 17 - 19 - 20 - 14 illustrates the great difficulty of assigning a meaningful value to ν_{eq}. Thus if a straight line skeleton from 0 to 15 is assumed, ν_{eq} will be close to unity, but if the straight line 0 to midway between 14 and 15 is used, ν_{eq} drops to 0.27, a ridiculously low value for the situation.

Figures 5a, b, and c show ϕ - δ plots for the bi-linear joint with slopes of unity and one fifth. The areas of the frictional loops do not differ greatly from the corresponding numbered ones of Figures 3a, b, and c, but the areas under the skeletons passing through the origin are significantly larger than before, consequently the eq values will be appreciably lower.

RELATION OF EXPERIMENTAL RESULTS TO THE IDEALIZED CONSTRUCTION

The previously mentioned report on friction joints by Pian, Hallowell and Bisplinghoff[2] is a highly analytical study of the basic mechanism of damping in built-up structures. It is also supported by well designed experiments. The authors conclude that:

a) the main source of damping is the slippage in the joint; the internal friction of the material contributes very little effect.

b) the energy loss depends only on the amplitude of vibration, but not on the absolute value of stress.

c) the energy loss per cycle varies approximately as the third power of the load amplitude.

d) the energy loss is approximately in inverse proportion to the tightness of the screw joints.

e) the hysteresis loop closes itself after the first complete load cycle.

f) the surprisingly small friction slippage in the joint is mainly confined to the region of the first and second screw clamping out of a possible 18 clampings.

Figure 6a shows a replot of their test results on the basis of unit slope of the tangent to the presumably primitive curve at the origin. It indicates clearly that circular arcs are excellent approximations for the ϕ - δ relationship, and that the assumption of unit return slopes at the return points is realistic. However, it does not show that the return trajectories pass precisely through the two antisymmetrical points on the primitive curve. A small discrepancy ε exists; this is possibly due to the curve not being a primitive one. The authors are very insistent that initial, locked-up stresses influence the first trajectory appreciably.

In Figure 6b two of the authors' curves have been replotted on the basis of unit slope for the skeletons. The results again indicate that circular arcs are good representations of the trajectories and that only the load amplitudes and not the absolute load values govern the size of the hysteretic loop.

The area A enclosed by two circular segments of equal radius ρ is equal to:

$$A = 2\rho^2(\psi - \tfrac{1}{2}\sin 2\psi)$$

in which ψ is the half angle subtended by the intersecting arcs. Since the length R of the common cord of the intersecting arcs is $2\rho \sin\psi$ we have:

$$A = \tfrac{1}{2}R^2 \frac{\psi - \frac{1}{2}\sin 2\psi}{\sin^2\psi}$$

If we restrict the half angle ψ to small values, the first approximation becomes:

$$A \approx \tfrac{2}{3}\psi R^2 \approx \tfrac{1}{3}\frac{R^3}{\rho}$$

Considering that the length R of the cord is proportional to the square root of the sum of the squares of the ϕ and δ ranges, it is clear that for ρ constant the frictional work will be approximately proportional to the third power of either the deformation and/or load ranges. Since the experiment indicated this to be the case, it constitutes an additional argument in favor of using circular trajectories.

One of the most important experimental studies of welded joints was published as early as 1933 by Professor Rio Tanabashi[3]. Figure 7 shows a replot of the largest loop, i.e. the i_1, i_2 j_1 cycles of his curve numbered 25. Unit slope was given to the skeleton of the loop rather than to an initial slope at the origin because it was judged that the joint might not have been in a primitive condition after so much experimentation. It is seen that in spite of the relatively large loads and angular deformations, the circular trajectories give a fair representation. Note that the initial slopes of the return trajectories are almost identical with the slope at the origin.

As a third example of excellent experimental work on very composite joints we consider the work of K. Takeyama and K. Goto[4] who tested a prefabricated, reinforced concrete, two story building in 1947. A copy taken from the authors' Figure 1.10 is shown in our Figure 8. It is apparent that the curvatures of the segments are not constant, being greater at the ends than at the middle.

JOINTS THAT SOFTEN GRADUALLY

In order to explain the smaller curvature at the middle of the trajectories, we consider the plots shown in Figure 9. In this case the assumed primitive curve is linear between $\delta = \pm 1$, but for larger values of δ it is made to be circular reaching zero slope at $\delta = \pm 7$. On the geometrical principles of: initial return slopes of unity, and all circular trajectories passing through the "elastic limit" points at $\delta = \pm 1$, the family of curves can be drawn without much effort. The resulting cusps at the positive and negative invariant points clearly are not to be expected in experimental work, instead a straightening of the trajectories or even a curvature change near their middles may occur.

JOINTS THAT STIFFEN GRADUALLY

So far we have not considered the joints that stiffen. In this case the geometrical principles assumed to relate to softening joints must be modified considerably. Since the initial slope at the origin is smaller than subsequent slopes, it will not be possible to assume that the return trajectories will start with initial unit slopes. We shall still retain the idea of constant radius circular trajectories, but the magnitude of their radii will be determined by new and debatable geometrical rules.

Figure 10 depicts a family of ϕ , δ curves relating to a primitive curve which is linear between $\delta = \pm 1$ and curvilinear for values of greater than ± 1. For the sake of simplicity the curved part is made circular and we exclude from consideration the infinite slope situation. In this case the primitive curve is assumed to be a skeleton. If the two lines a-a and b-b are drawn normal to the original slope through points $\phi = \delta = \pm 1$, the centers of all the circular trajectories as well as those of the two circular branches of the primitive curve will fall on either one or the other of these lines. Thus, referring to the largest curve, whose tip point is located at $\delta = 5$, we note that the center of the primitive curve's circular branch is located on line b-b at c, while the center of the trajectory 1 - 2 is located on line a-a at d, where the extended radius 1-c cuts line a-a. The radius ρ is therefore equal to d - c - 1. Moreover, the circular trajectory from 1 - 4 has the same radius ρ but its center is located on the line b-b at e. Trajectories 2 - 3 and 3 - 4 also have the constant radius ρ , but their centers are now located on the line a-a and b-b respectively. The intersection of the trajectories at stations 2 and 4 will create cusps.

Hysteretic loops for tip locations at $\delta = \pm 4$, ± 3, and ± 2 have been shown. It is felt that improvements in the construction procedure for the ϕ - δ relations of stiffening joints are indicated.

DETERIORATING JOINTS

It would not be reasonable to exclude from this discussion joints that show some deterioration. Thus, any reinforced concrete structure is in the fullest sense a system of many joints between reinforcement and concrete. Since cracks are likely to be present initially or to occur for various

reasons, the possibility of a deterioration is ever present.

About 10 years ago Dr. K. Muto[5] experimented with alternate plus and minus loadings on reinforced concrete panels. He observed a gradual deterioration and explained its relative slowness by including a hypothetical curve depicting the resistance of a bare reinforcement system.

Wilbur and Hansen[1] at about the same time performed their static and dynamic tests on reinforced concrete beams. They also called attention to the fact that the resistance of the beams to the first reverse loading is only slightly impaired by the sizable cracks produced by the first direct loading. Unfortunately their experiments did not take the beams through more than one cycle. The average ϕ - δ curve of seven "supposedly identical" beams, is shown in Figure 11. It is seen that the geometrical construction technique : employing circular trajectories - unit return slopes - pass through yield points, represents the first complete cycle fairly well.

Riveted joints were carefully studied as early as 1935 by Dr. Tanabashi[6] He subjected numerous specimens, some of them with as many as 120 rivets, to alternate plus and minus static loads. One of Dr.Tanabashi's curves, the C_9 - C_{10} loop of 15 (Bs), has been replotted in Figure 12 on the basis of unit slope of the main diagonal or skeleton. In this case the deterioration is remarkably small as is evident by the exceptionally fine closure at point C. If we assume a skeleton as shown by the dotted line, the ν_{eq} becomes approximately 0.23.

Dr. Tanabashi explains the shape of his ϕ - δ curves by describing two idealized ϕ - δ models, one due to Masing and the other of his own invention. This later model may be termed a slip model; it explains the effect produced by a slip of the rivets in their holes, especially after the holes have suffered permanent deformations.

Jacobsen[7] also devised a behavioristic model comprising a multiplicity of St.Venant elements in series to illustrate the hysteretic performance of joints. In this case a crude mechanism was proposed to represent, but not to explain, the progressive deterioration aspect.

HIGHLY NON-LINEAR DETERIORATION JOINTS

A couple of years ago Professor K. Kaneta and the author[8] experimented on simple nailed joints in alternating static loadings of up to as many as 31 cycles. Figure 13 shows an experimental, automatically recorded test on a shear joint involving only two pairs of nails. It is seen that up to a load of about ± 150 pounds the reversed curvature effect is not very distinct. At +175 pounds a repetition of the plus load shows deterioration, and as the load increases further, the reversed curvature becomes more and more pronounced. Five half cycles from 0 up to 275 pounds clearly shows a deterioration which does not progress much faster than it did for the changes from 0 to 175 pounds. The subsequent reversal of load to -275 pounds exhibits the sway-backed effect also recorded by Dr.Tanabashi's riveted joint experiments. Four half cycles from 0 to -275 pounds still

indicate a ...ably slow deterioration. The final reversal to +325 pounds calls for a δ range of 0.37 inches and is followed by a rapid distortion leading to a final load of approximately 360 pounds.

There can be no doubt that the slip model invented by Dr. Tanabashi explains the almost horizontal parts of the ϕ - δ curves. The subsequent increases in load and extremely rapid reductions when δ is diminished are probably due to a change in clamping pressure, effected by the tension in the nails, induced by the nail head action. The tests show conclusively that Coulomb or rubbing friction between the wood surfaces deteriorates very slowly and is responsible for a large amount of damping.

An alternating shear test on a square panel involving a hinged 2" x 4" lumber frame and two ¼" Ply wood panels is depicted in Figure 14. Notice that the alternating load progresses at regular load increments of 50 pounds and that the scales of the two diagrams differ. The smaller plot on the left actually fits into the central "hole" of the larger diagram. It is remarkable that the curves relating to this composite joint, involving 20 pairs of nails, follow closely the curves for the simple joint with only two pairs of nails.

Figures 15 and 16 represent the ±1000 pound and the ±2450 pound cycles of Figure 14, plotted on the basis of unit slope of their tip to tip diagonals. It is clearly seen that logical skeletons should be of the rising type. A second degree and a fifth degree parabolic skeleton are indicated by the dotted lines. In these cases however, the significance of an equivalent viscous damping is questionable.

CONCLUSIONS

1.) The primary object of the study has been to gain some understanding of the hysteretic type of damping encountered in composite structures. Special consideration has been devoted to idealized, non-deteriorating structural joints in which elastic-plastic deformations as well as rubbing friction give rise to energy dissipation.

2.) A discussion of the concept of equivalent viscous damping has led to the conclusion that its practical justification is valid in many cases, but that for pure, highly non-linear restorations as well as for large values of non-viscous types of damping the concept becomes almost meaningless. An imperfect relationship between the equivalent viscous damping ratio ν_{eq}, the hysteretic work area, and the area under a "skeleton" curve is discussed, and its use is advocated.

3.) An idealized, geometrical procedure for representing load-distortion relations of non-deteriorating joints has been developed. It involves a non-dimensional plotting by which area distortions are minimized. The geometrical principles advocated for constructing the load-distortion plots involve the use of circular trajectories whose centers and radii are geometrically related to the initial unit slope and to the antisymmetrical location of two invariant yield points.

4.) The curves resulting from the suggested geome... onstruction procedure have been compared with some experimental da..., and the variance between them has been discussed. It is felt that the variances are not so great as to render the suggested construction procedure useless, but it must be tempered with caution as well as with experience if it is used for predicting damping values . Its usefulness is in an analytic sense rather than in a synthetic one.

5.) Deteriorating joints are considered briefly, and only from a factual point of view. It is concluded that in some cases deterioration takes place remarkably slowly. Alternating static loading tests repeated for several cycles seem, at the present, to be the approach most likely to have practical value. Dynamic loadings are difficult to devise, record and analyze because it is almost impossible to deal effectively with time dependent properties of the composite materials.

REFERENCES

(1) "Behavior of Structural Elements Under Impulsive Loads, I and II." A report submitted to New England Division, Corps of Engineers, in partial completion of Contract No. DA-19-016-eng-239 by J.B.Wilbur and R.J.Hansen, MIT., November 1950.

(2) "Investigation of Structural Damping in Simple Built Up Beams," Contract Report on ONR Project NR-035-259 at MIT by THH Pian, F.C.Hallowell, Jr. and R.L.Bisplinghoff.

(3) "Static Tests of Welded Joints of Steel Structures Subjected to Alternate Bending Moments," Journal of Japanese Society of Welding, Vol.9, No.12, 1933, by Rio Tanabashi (in Japanese).

(4) "Tests of the Ultimate Strength of a Prefabricated Reinforced Concrete Building." Building Research Institute, Ministry of Construction, Tokyo, 1947 by K. Takeyama and K. Goto (in Japanese).

(5) "Investigation of Earthquake Resistant Walls." Proceedings of Architectural Institute of Japan, 1950-51 by K. Muto, Tokyo University (in Japanese).

(6) "Tests to Determine the Behavior of Riveted Joints of Steel Structures under Alternate Bending Moments," Memoirs of College of Engineering, Kyoto Imperial University, 1935. Vol. VIII, No. 4 by Rio Tanabashi (in English).

(7) "Behavioristic Models Representing Hysteresis in Structural Joints"; Laboratoriet for Bygningsteknik, Danmarks Tekniske Højskole, Meddelelse Nr. 10, pp. 126 -138 Copenhagen 1959, by Lydik S. Jacobsen.

(8) "Study of Structural Damping and Stiffness in Nailed Joints," Engineer's Thesis at Stanford University, Sept. 1958 by Kiyoshi Kaneta.

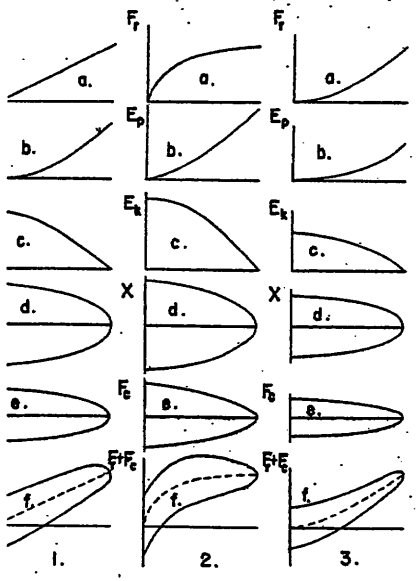

FIGURES 1, 2, 3: RESTORING FORCES, ENERGIES, VELOCITIES, DAMPING FORCES AND TOTAL FORCES FOR A LINEAR, A SOFTENING AND A HARDENING VIBRATORY SYSTEM.

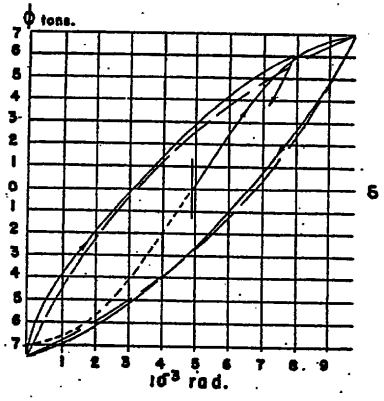

FIGURE 7: EXPERIMENTAL CURVE FROM REFERENCE (3) WITH CIRCULAR ARC APPROXIMATION. BASED ON DIAGONAL SKELETON $\gamma_{eq} \approx 0.16$.

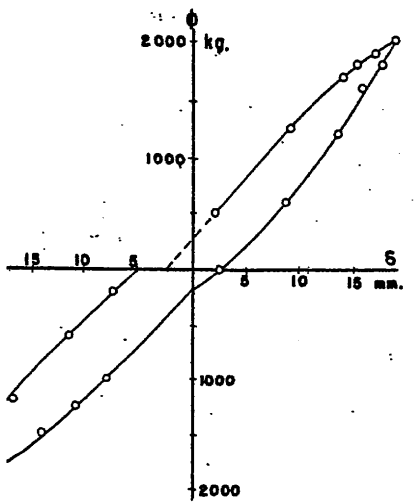

E 8: ϕ-δ RELATIONS OF A PRECAST REINFORCED CONCRETE TORY BUILDING. REFERENCE (4) $\gamma_{eq} \approx 0.085$.

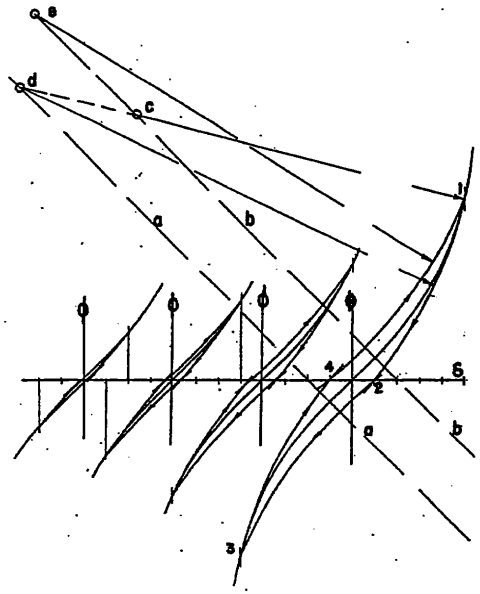

FIGURE 10: SUGGESTED ϕ-δ CONSTRUCTION OF A HARDENING JOINT. $\gamma_{eq} \approx 0.020, 0.030, 0.050, 0.075$.

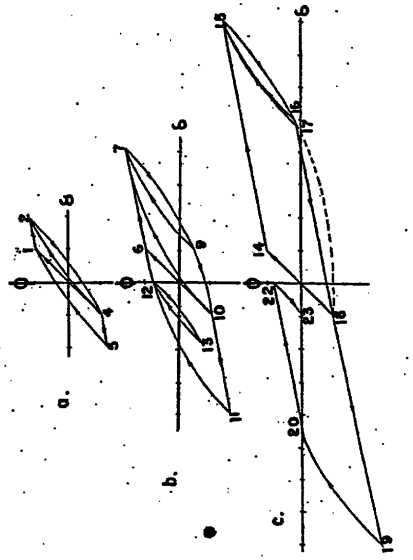

FIGURE 9: IDEALIZED CONSTRUCTION OF ϕ-δ RELATIONS IN A RECTILINEAR JOINT WITH SLOPES OF UNITY AND ONE FIFTH.

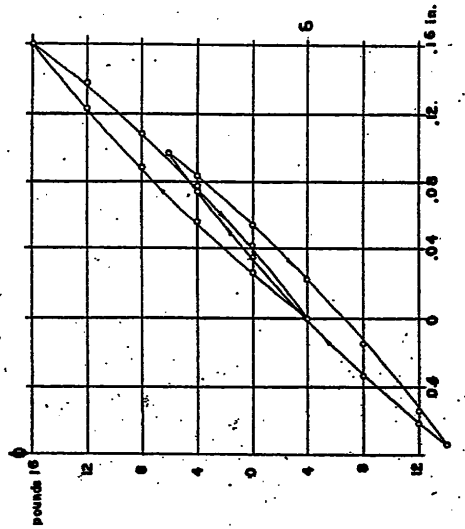

FIGURE 10a: CONSTANT CURVATURE ϕ-δ RELATIONS WITH EXPERIMENTAL POINTS OBTAINED BY REFERENCE (3). γ_{eq} INDEPENDENT OF AMPLITUDE LOAD. REFERENCE (3). $\gamma_{eq} \approx 0.16$.

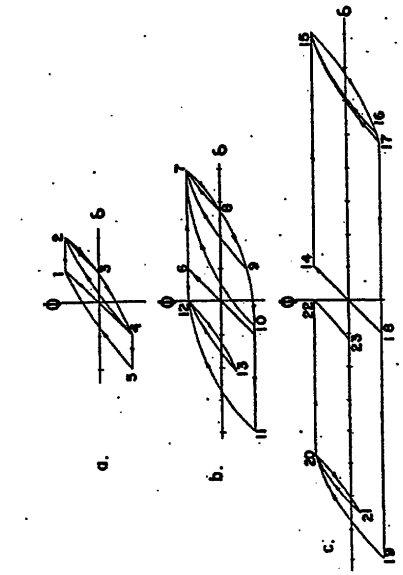

FIGURE 8: IDEALIZED CONSTRUCTION OF ϕ-δ RELATIONS IN A RECTILINEAR JOINT WITH SLOPES OF UNITY AND ZERO.

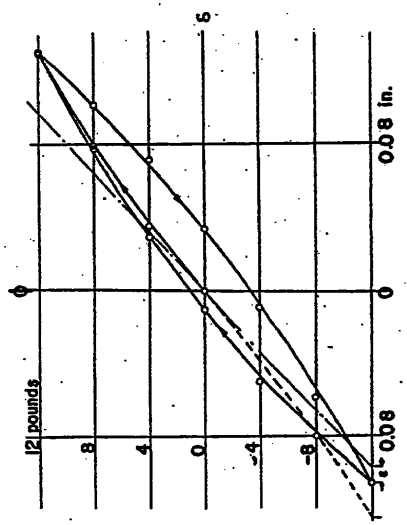

FIGURE 10b: CONSTANT CURVATURE ϕ-δ RELATIONS WITH EXPERIMENTAL POINTS OBTAINED BY REFERENCE (3). BASED ON DIAGONAL SKELETON, $\gamma_{eq} \approx 0.16$.

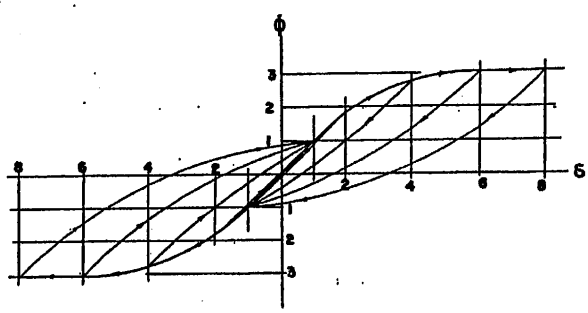

FIGURE 9: SUGGESTED IDEALIZED CONSTRUCTION OF THE Φ-δ RELATIONS OF A SOFTENING JOINT.

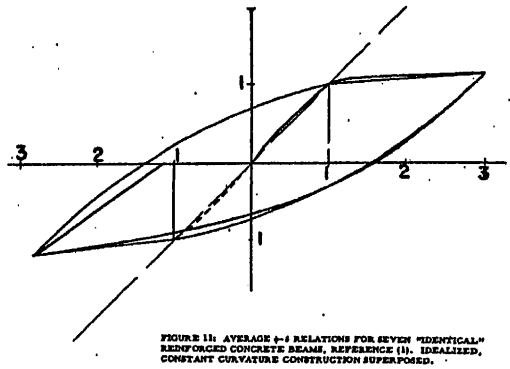

FIGURE 11: AVERAGE Φ-δ RELATIONS FOR SEVEN "IDENTICAL" REINFORCED CONCRETE BEAMS, REFERENCE (1). IDEALIZED, CONSTANT CURVATURE CONSTRUCTION SUPERPOSED.

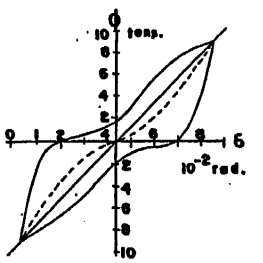

FIGURE 12: Φ-δ RELATIONS OF A RIVETED JOINT SHOWING REVERSE CURVATURE. REFERENCE (6). WITH 3/2 POWER PARABOLIC SKELETON, $\nu_{eq} \approx 0.22$.

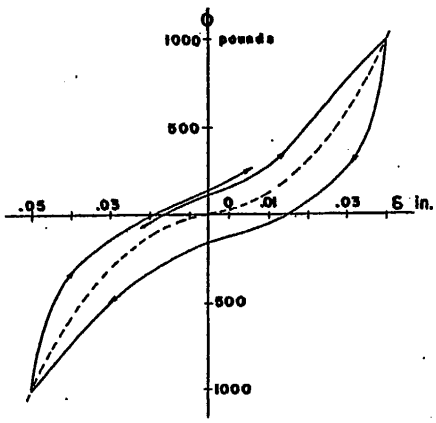

FIGURE 13: Φ-δ RELATION OF ± 1000 POUND CYCLE OF FIGURE 14. WITH SECOND DEGREE PARABOLIC SKELETON, $\nu_{eq} \approx 0.18$.

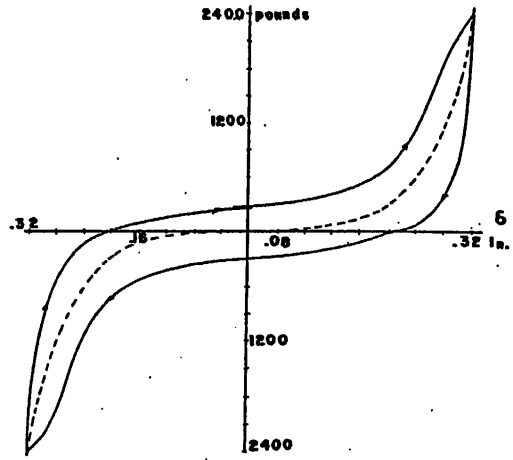

FIGURE 14: Φ-δ RELATION OF ± 2400 POUND CYCLE OF FIGURE 14. WITH FIFTH DEGREE PARABOLIC SKELETON, $\nu_{eq} \approx 0.12$.

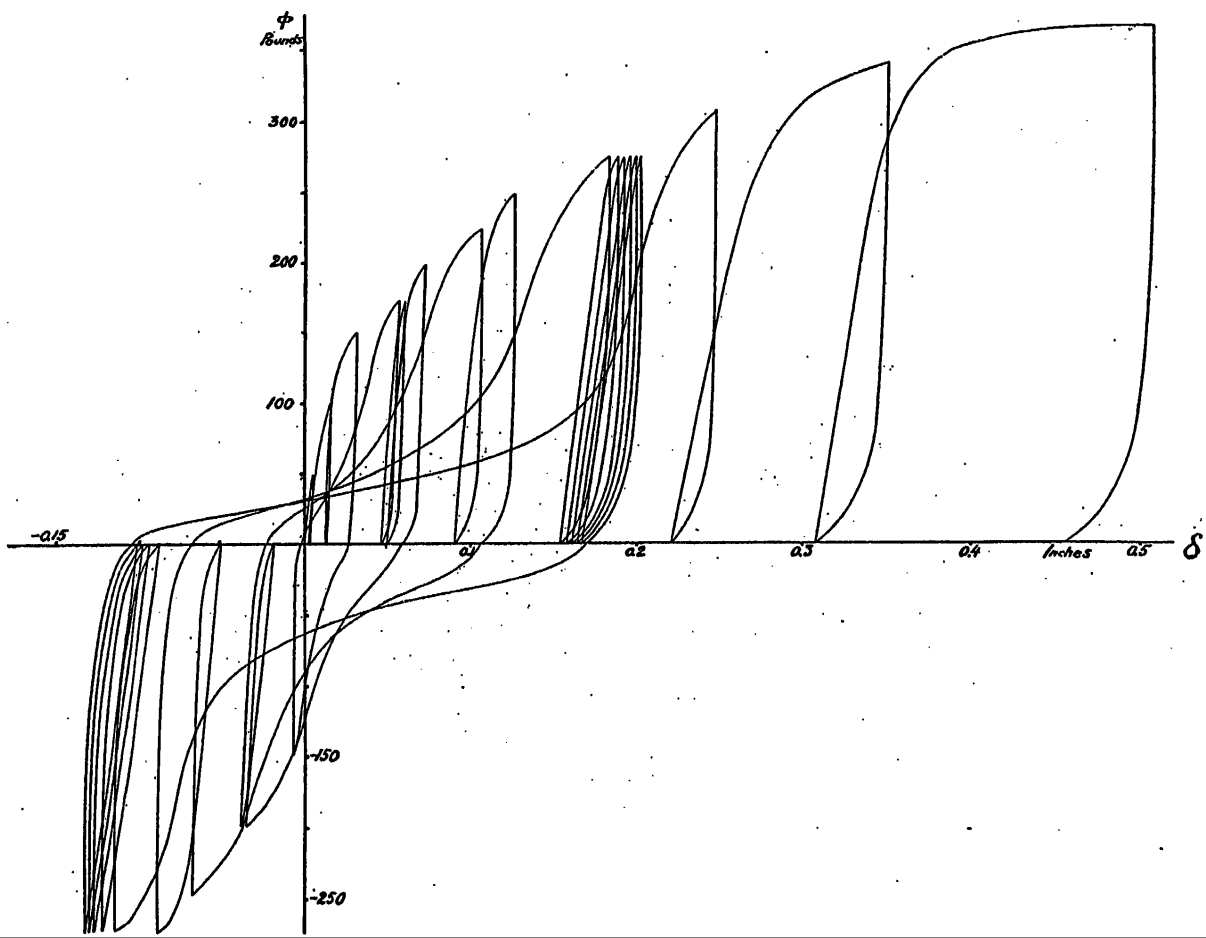

FIGURE 15: EXPERIMENTAL LOAD DISTORTION RELATIONS OF A SIMPLE JOINT USING TWO PADS OF HAIR. REFERENCE (9).

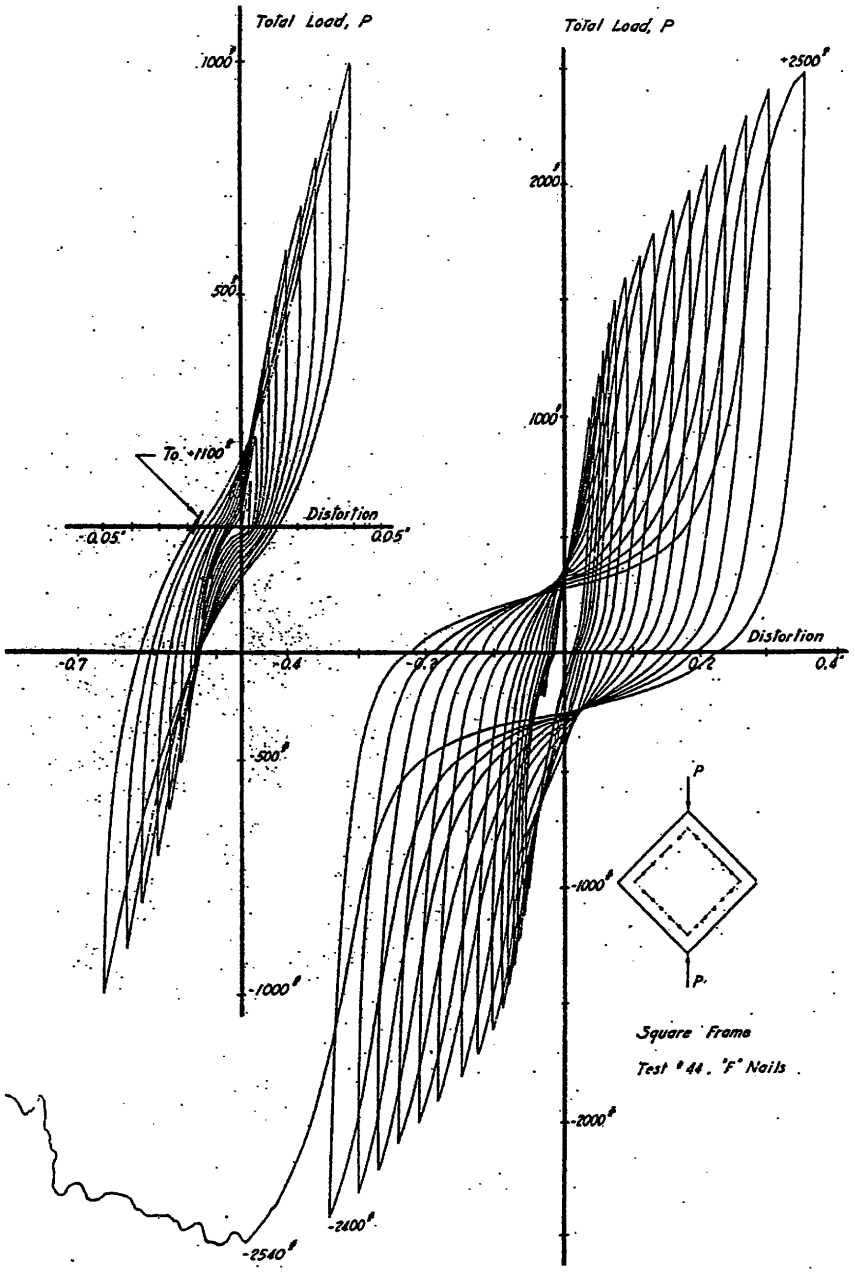

FIGURE 14: EXPERIMENTAL LOAD DISTORTION RELATIONS OF A HINGED FRAME STIFFENED BY PLYWOOD PANELS AND USING TWENTY PAIRS OF NAILS. REFERENCE (8).

NONLINEAR VIBRATIONS OF BUILDING STRUCTURES

BY NORIHIRA ANDO[1)]

PREFACE

The dynamical force-displacement relation of a building is complicated in its dependency on the number of repetition of the displacement as well as on the magnitude of displacement and velocity. Hence, there are many difficulties in the prediction of the effective rigidity and the damping of a building structure in a state of violent motions due to a strong motion earthquake. In spite of the development of the response spectrum techniques, one of difficulties seems to be in this respect in introducing a substantial design basis from the studies based upon them.

A building structure producing a large deflection beyond its elastic limit is generally recognized as a hysteretic system. Though the dynamical properties of restoring force of a building structure is complicated and have many varieties, some typical hysteretic forms of the force-displacement relation may be assumed. The response computing techniques for the nonlinear systems must be developed, for which the fundamental theoretical basis will be desirable.

In this paper, studies on vibrating systems with some typical forms of the hysteretic force-displacement relations are presented. In Chap. I, theory of stationary vibrations of hysteretic single degree of freedom systems is treated. In Chap. II, solutions of transient vibrations of the hysteretic bilinear single degree of freedom systems are shown. In Chap. III, a method to discriminate the stability of the stationary vibrations of hysteretic single degree of freedom systems is given. The discriminant of the stability are explicitly obtained about the systems treated in the previous chapters. In Chap. IV, the transient vibrations of hysteretic bilinear two degrees of freedom system are solved.

CHAPTER I
FORCED STATIONARY VIBRATIONS OF HYSTERETIC SINGLE DEGREE OF FREEDOM SYSTEMS

1.1 Equation of motion

Let the force-displacement relation for the forced stationary vibrations of a single degree of freedom structure be as shown in Fig. 1. The equation of motion for a vibration excited by a stationary harmonic force is, for non-negative velocity,

$$(1.1)\quad m\frac{d^2y}{dt^2} + f(y,a) = -P\cos(pt+\phi)$$

where ϕ is the phase angle between the force and the displacement. The spring stiffness for a small displacement is

$$(1.2)\quad c = \left[\frac{\partial f(y,a)}{\partial y}\right]_{y=0,a=0}, \quad \text{from which } \omega = \sqrt{\frac{c}{m}}$$

1)Assist. Prof. of Structural Engineering, Yokohama National University, Yokohama, Japan